

Strain induced phase separation in $\text{La}_{0.67}\text{Ca}_{0.33}\text{MnO}_3$ ultra thin films

V. Peña^a, Z. Sefrioui^a, D. Arias^a, C. León^a, J. Santamaria^{a,*}, M. Varela^b, S.J. Pennycook^b,
M. Garcia-Hernandez^c, J.L. Martinez^c

^a *GFMC, Departamento de Física Aplicada III, Universidad Complutense de Madrid, 28040 Madrid, Spain*

^b *Condensed Matter Science Division, Oak Ridge National Laboratory, Oak Ridge, Tennessee 37831-6031, USA*

^c *Instituto de Ciencia de Materiales de Madrid (ICMM-CSIC), 28049 Cantoblanco, Madrid, Spain*

Abstract

Magnetic and transport properties are investigated in epitaxial $\text{La}_{0.67}\text{Ca}_{0.33}\text{MnO}_3$ thin films grown on SrLaAlO_4 under high in plane compressive strain (-3.1%). Films with thickness in the range 2–6.5 nm show a two dimensional coherent growth mode and are significantly strained as shown by the expansion of the out of plane lattice parameter. We provide evidence for phase separation induced by the inhomogeneous strain field, free of artefacts related to composition changes at grain boundaries or structurally disordered regions characteristic of island growth. © 2005 Elsevier Ltd. All rights reserved.

Keywords: A. Manganites; D. Colossal magnetoresistance; D. Strain; D. Phase separation

1. Introduction

The complex interplay between the spin, lattice and charge degrees of freedom in colossal magnetoresistance (CMR) manganites is responsible for the inhomogeneous ground state with metallic and insulating regions competing at nanometer and micrometer length scales [1,2]. The large sensitivity of the physical properties of these compounds to small perturbations (magnetic fields, X-rays, etc.) results of metallic phases being converted into insulating or vice versa, supporting the existence of metastable phases. There is solid theoretical and experimental evidence for this phase separation (PS) picture of the manganese oxides, although its ultimate origin remains not well understood.

There have been recent reports outlining the importance of long-range lattice strains for the understanding of the PS scenario [3,4]. Lattice distortions may be related to oxygen displacements or to Jahn-Teller distortion around e_g localized electrons in Mn^{3+} octahedra [5]. Distorted octahedra may stack differently in- and out of plane giving rise to short and long wave length lattice distortions. These lattice distortions have been proposed to be at the origin of the energy landscape responsible of the inhomogeneous ground state [3]. On the other hand distortions of the MnO_6 octahedra resulting of the

replacement of the trivalent La ions by divalent Ca have been proposed to have a cooperative nature which also yields PS in 3D models [4]. In connection to these models, epitaxial strain in ultrathin films may help in providing a firmer footing to the role of lattice distortions in PS phenomena. There has been substantial work in the past dealing with modified properties of thin films with thickness [6–8], but structural disorder at the first stages of the growth and/or island growth does not allow to distinguish genuine strain effects from composition changes at disordered regions. In this paper we present results of ultrathin $\text{La}_{0.67}\text{Ca}_{0.33}\text{MnO}_3$ films grown on SrLaAlO_4 ($a=0.375$ nm) under high in plane compressive strain (-3.1%). This substrate has an in plane lattice parameter similar to LaAlO_3 ($a=0.378$ nm), but without the twin structure responsible for island growth in LaAlO_3 [9]. We show 2D dimensional, epitaxial growth below the critical thickness what allows exploring the effect of lattice distortions on the PS in highly ordered films with thickness in the 2–6.5 nm range. We have found evidence for the presence of insulating regions coexisting with ferromagnetic metallic ones, which most likely originate at an inhomogeneous strain field at the critical thickness.

2. Experiment

$\text{La}_{0.67}\text{Ca}_{0.33}\text{MnO}_3$ (LCMO) ultra thin films were grown in a high-pressure sputtering system (3.4 mbar), and high temperature (900 °C). This provides a very thermalized and ordered growth at a slow rate (0.02 nm/s) which allows an accurate control of the layer thickness. Substrates were (001) oriented

* Corresponding author. Tel.: +34 913944367; fax: +34 913945196.
E-mail address: jacsan@fis.ucm.es (J. Santamaria).

SrLaAlO₄ (SLAO) with a tetragonal structure ($a=b=0.375$ nm, $c=1.263$ nm).

The out of plane parameter of the LCMO thin films was obtained from X-ray diffraction. Reflectivity oscillations at low angle were used to determine sample thickness. Z-contrast images were performed in a VG Microscope HB501UX scanning transmission microscope (STEM) operated at 100 kV with field emission gun. This microscope is equipped with a Nion aberration corrector, which provides a spatial resolution close to 0.1 nm for imaging. Cross-section samples for STEM were prepared by conventional grinding, dimpling and ion milling with Ar ions with energy of 5 kV, at an incident angle of 8°.

3. Results and discussion

A set of thin films with thicknesses comprised between 2 and 37 nm were grown on SLAO substrates. Fig. 1a shows high angle X-ray diffraction spectra for different samples. Note that upon thickness reduction the width of the LCMO (002) diffraction peak increases substantially and that the peak shifts to smaller angles. The FWHM of the Bragg peak can also be used to estimate layer thickness using Scherrer's formula. The out of plane lattice parameter obtained from the position of the (002) Bragg peak for the different films is plot as a function of thickness in Fig. 1b. The pronounced increase of the out of

plane lattice parameter for sample thickness below 9 nm evidences a high degree of epitaxial strain. This can be understood according to Poisson effect in view of the large (−3.1%) in plane lattice mismatch between LCMO and SLAO (in plane compression causes out of plane expansion). These data suggest a 9 nm critical thickness for strain relaxation although some residual strain remains up to 37 nm thick films for which bulk lattice parameters are approached.

STEM images (Z-contrast) of highly strained (6.5 nm) and partially relaxed (9 nm) films show coherent growth, with flat interfaces between film and substrate (see Fig. 1c and d). The STEM image of the highly strained 6.5 nm film evidences a very coherent two dimensional growth mode (Fig. 1c) while the partly relaxed 9 nm thick film shows island growth (Fig. 1d). These images, together with the evolution of the c parameter with thickness, confirm that the growth mechanism for LCMO films under compressive strain is of the Stranski–Krastanov type, where a ‘wetting-layer’ grows first on the substrate followed by the nucleation of coherent islands on top of the wetting layer above the critical thickness. Relaxation results of the stored elastic energy being larger than the interface energy saved by the atom-on-atom coherent growth. If sample thickness is further increased islands are over grown eventually yielding flat sample surfaces for thickness in excess of 50 nm as evidenced by atomic force microscopy observations (not shown). This result outlines that studies on the

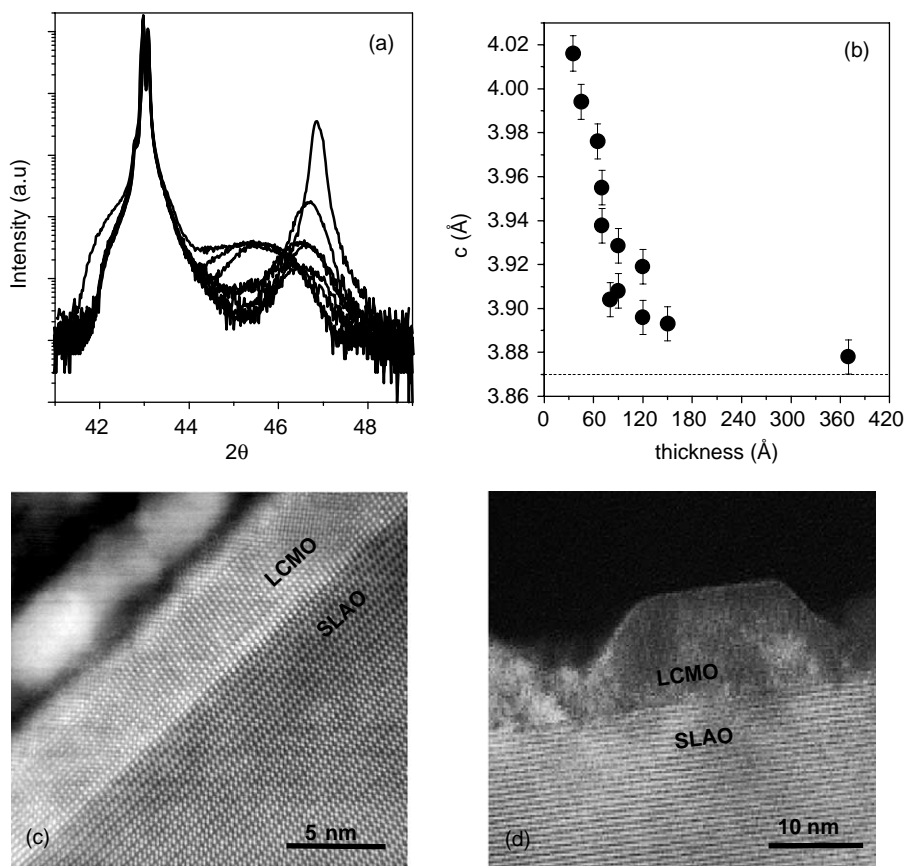


Fig. 1. (a) XRD high angle pattern of LCMO thin films of different thicknesses (37, 15, 12, 9, 8, 6.5, 4.5 and 3.5 nm) grown on SLAO (001) oriented substrate. (b) c parameter vs. thickness of LCMO films (broken line represents the bulk value). (c) STEM image of a 6.5 nm LCMO thin film. (d) STEM image of a 9 nm LCMO film.

effect of epitaxial strain require the growth of samples with thickness well below the critical thickness, since compositional disorder at the edges of the terraces or islands may affect doping and thus obscure the effect of PS as discussed below.

Fig. 2 displays the evolution of the metal insulator transition (MIT) from resistance measurements for samples with different thickness. For the partially relaxed (thicker) films, the MIT occurs at a temperature close to the value reported for bulk LCMO (~ 250 K). For the highly strained (thinner films), on the other hand, the transition shifts to lower temperatures (~ 130 K, for 6.5 nm) while 4.5 nm films (or thinner) remain insulating. Note that the shift of the MIT occurs only below the critical thickness. Sample magnetic moment was also found to decrease for thicknesses below the critical value. Fig. 3 shows hysteresis loops for 2.5, 4.5, 6.5 and 9.0 nm thick samples. Note that even the very thin samples are ferromagnetic although a decrease in M_{sat} is found. In addition the temperature dependence of the magnetization shows the onset of a ferromagnetic transition close to 240 K for the 4.5 nm film (see inset of Fig. 3). This suggests the presence of insulating (resistance) and ferromagnetic (SQUID) phases coexisting in the strained samples. In order to further investigate this, we have done magnetoresistance measurements in the 4.5 nm film in up to 16 T magnetic fields applied parallel to the layers (see Fig. 4). The Arrhenius plots of Fig. 4 evidence a pronounced decrease of the resistance with applied magnetic field. Moreover, the resistance curve under 16 T field displays a hump characteristic of the metal insulator transition at a temperature close to 250 K, which coincides with the onset of the ferromagnetic transition obtained from magnetization measurements (see inset of Fig. 3). Inset in Fig. 4 shows magnetoresistance measurements as a function of magnetic field at various temperatures. A large magnetoresistance is

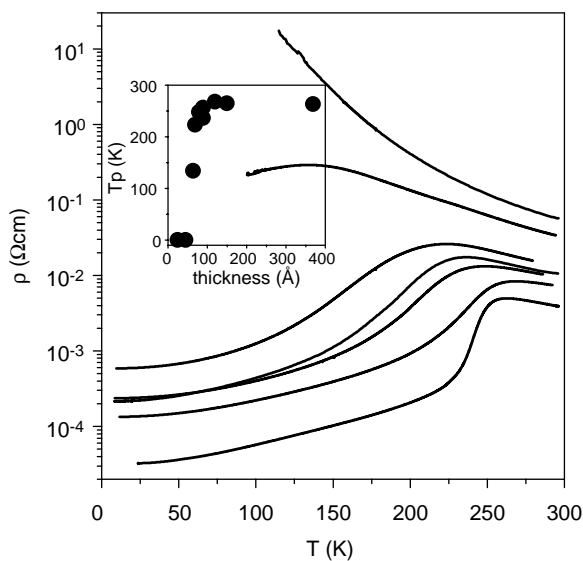


Fig. 2. Resistivity vs. temperature for a set of LCMO thin films (from top to bottom: 4.5, 6.5, 7, 8, 9, 12 and 37 nm). Inset shows the temperature of the peak T_p vs. thickness.

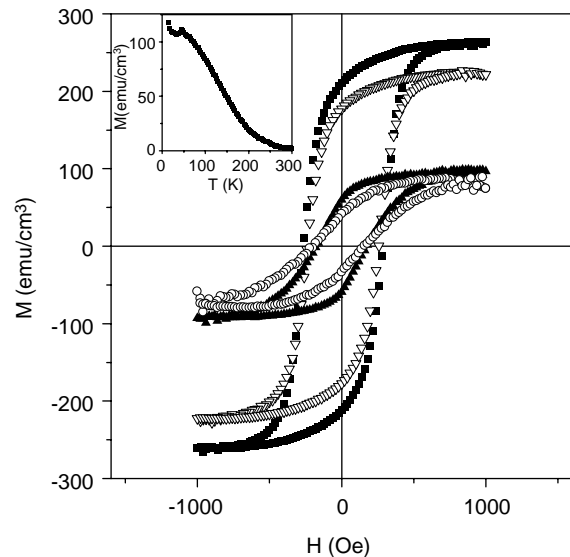


Fig. 3. Hysteresis loops for (■) 9, (▽) 6.5, (▲) 4.5 and (○) 2.5 nm, measured at 50 K and field applied parallel to the layers. Inset shows the temperature dependence of the magnetization of 4.5 nm film.

found for this insulating sample, which increases when temperature is lowered. Notice also that there is significant magnetoresistance (30%) at room temperature, that is, well above the MI transition of the relaxed samples. The PS picture of an inhomogeneous sample with coexisting insulating and ferromagnetic metallic phases emerges naturally, where the insulating phase is driven metallic by applying a magnetic field. Transport data are thus explained by percolative transport through the ferromagnetic regions, whose size is controlled by the applied magnetic field.

In summary, the analysis of epitaxial 2D strained films provides direct evidence of PS triggered by the inhomogeneous

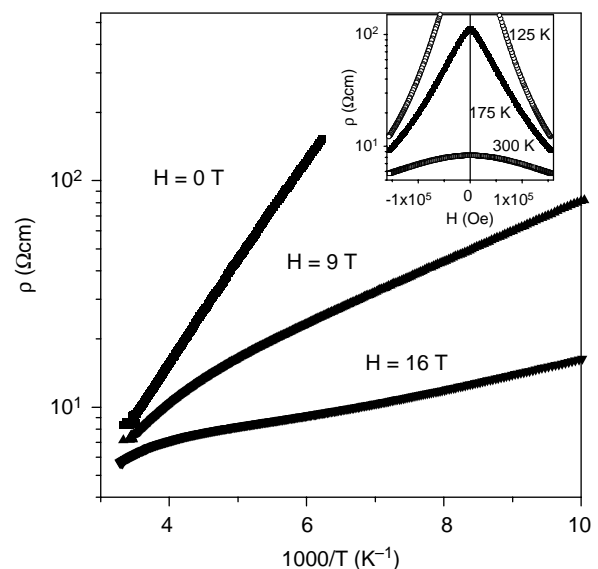


Fig. 4. Resistivity vs. temperature for the 4.5 nm film, for $H=0$ T (■), for $H=9$ T (▲) and $H=16$ T (▼), applied parallel to the layer. Inset shows magnetoresistance curves at different temperatures, 125 K (○), 175 K (■) and 300 K (□).

strain field at strain relaxation, outlining the importance of electron lattice coupling in the phase separation picture in agreement with recent theoretical studies.

Acknowledgements

Work supported by MCYT MAT 2002-2642 and CAM 07N/0032/2002, UCM PR3/04-12399 and Fundación Ramón Areces.

References

- [1] E. Dagotto, T. Hotta, A. Moreo, Colossal magnetoresistant materials: the key role of phase separation, *Phys. Rep.* 344 (2001) 1.
- [2] M.B. Salamon, M. Jaime, The physics of manganites: structure and transport, *Rev. Mod. Phys.* 73 (2001) 583.
- [3] K.H. Ahn, T. Lookman, A.R. Bishop, Strain-induced metal-insulator phase coexistence in perovskite manganites, *Nature* 428 (2004) 401.
- [4] J. Burgy, A. Moreo, E. Dagotto, Relevance of cooperative lattice effects and stress fields in phase-separation theories for CMR manganites, *Phys. Rev. Lett.* 92 (2004) 97202.
- [5] A.J. Millis, Lattice effects in magnetoresistive manganese perovskites, *Nature* 392 (1998) 147.
- [6] H.S. Wang, Qi Li, Kai Liu, C.L. Chien, Low-field magnetoresistance anisotropy in ultrathin $\text{Pr}_{0.67}\text{Sr}_{0.33}\text{MnO}_3$ films grown on different substrates, *Appl. Phys. Lett.* 74 (1999) 2212.
- [7] D.W. Abraham, R.A. Rao, C.B. Eom, J.Z. Sun, Thickness-dependent magnetotransport in ultrathin manganite films, *Appl. Phys. Lett.* 74 (1999) 3017.
- [8] R.A. Rao, D. Lavric, T.K. Nath, C.B. Eom, L. Wu, F. Tsui, Effects of film thickness and lattice mismatch on strain states and magnetic properties of $\text{La}_{0.8}\text{Ca}_{0.2}\text{MnO}_3$ thin films, *J. Appl. Phys.* 85 (1999) 4794.
- [9] A. Biswas, M. Raeswari, R.C. Srivasta, T. Venkatesan, R.L. Greene, A.J. Millis, Two-phase behavior in strained thin films of hole-doped manganites, *Phys. Rev. B* 61 (2000) 9665.